Molecular Cell Biology

Cancer Research

BRD4 Promotes Gastric Cancer Progression and Metastasis through Acetylation-Dependent Stabilization of Snail

Zhong-yi Qin[1], Tao Wang[1], Siyuan Su[2], Li-ting Shen[1], Guang-xi Zhu[1], Qin Liu[1], Liang Zhang[1], Ke-wei Liu[1], Yue Zhang[3], Zhi-hua Zhou[4], Xiao-ning Zhang[5], Liang-zhi Wen[1], Yue-liang Yao[5], Wen-jing Sun[1], Yan Guo[1], Kai-jun Liu[1], Lei Liu[1], Xing-wei Wang[1], Yan-ling Wei[1], Jun Wang[1], Hua-liang Xiao[6], Pengda Liu[2], Xiu-wu Bian[5], Dong-feng Chen[1], and Bin Wang[1,5]

Abstract

Cancer metastasis, a leading cause of death in patients, is associated with aberrant expression of epigenetic modifiers, yet it remains poorly defined how epigenetic readers drive metastatic growth and whether epigenetic readers are targetable to control metastasis. Here, we report that bromodomain-containing protein 4 (BRD4), a histone acetylation reader and emerging anticancer therapeutic target, promotes progression and metastasis of gastric cancer. The abundance of BRD4 in human gastric cancer tissues correlated with shortened metastasis-free gastric cancer patient survival. Consistently, BRD4 maintained invasiveness of cancer cells *in vitro* and their dissemination at distal organs *in vivo*. Surprisingly, BRD4 function in this context was independent of its putative transcriptional targets such as MYC or BCL2, but rather through stabilization of Snail at posttranslational levels. In an acetylation-dependent manner, BRD4 recognized acetylated lysine 146 (K146) and K187 on Snail to prevent Snail recognition by its E3 ubiquitin ligases FBXL14 and β-Trcp1, thereby inhibiting Snail polyubiquitination and proteasomal degradation. Accordingly, genome-wide transcriptome analyses identified that BRD4 and Snail regulate a partially shared metastatic gene signature in gastric cancer cells. These findings reveal a noncanonical posttranscriptional regulatory function of BRD4 in maintaining cancer growth and dissemination, with immediate translational implications for treating gastric metastatic malignancies with clinically available bromodomain inhibitors.

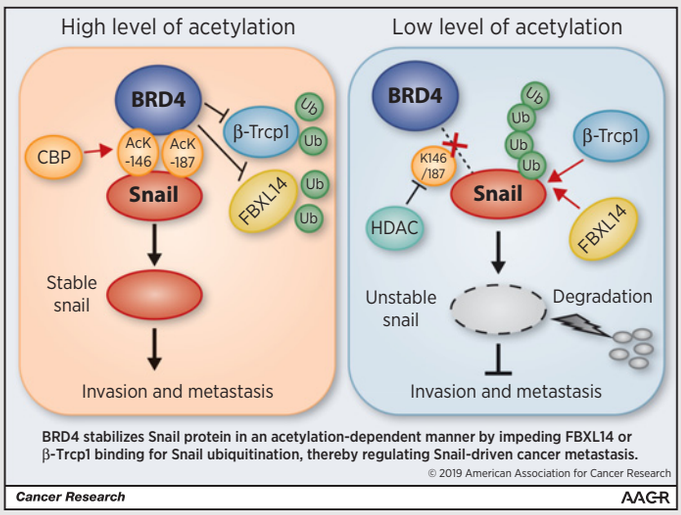

BRD4 stabilizes Snail protein in an acetylation-dependent manner by impeding FBXL14 or β-Trcp1 binding for Snail ubiquitination, thereby regulating Snail-driven cancer metastasis.

Cancer Research AACR

Significance: These findings reveal a novel posttranscriptional regulatory function of the epigenetic reader BRD4 in cancer metastasis via stabilizing Snail, with immediate translational implication for treating metastatic malignancies with clinically available bromodomain inhibitors.

Graphical Abstract: http://cancerres.aacrjournals.org/content/canres/79/19/4869/F1.large.jpg.

[1]Department of Gastroenterology, Daping Hospital, Army Medical University (Third Military Medical University), Chongqing, P. R. China. [2]Lineberger Comprehensive Cancer Center and Department of Biochemistry and Biophysics, The University of North Carolina at Chapel Hill, Chapel Hill, North Carolina. [3]Department of Oncology, Southwest Hospital, Army Medical University (Third Military Medical University), Chongqing, P. R. China. [4]Department of Pathology, The 904 Hospital of People Liberation Army, Wuxi, P. R. China. [5]Institute of Pathology and Southwest Cancer Center, and Key Laboratory of Tumor Immunopathology of Ministry of Education of China, Southwest Hospital, Army Medical University (Third Military Medical University), Chongqing, P. R. China. [6]Department of Pathology, Daping Hospital, Army Medical University (Third Military Medical University), Chongqing, P. R. China.

Z.-y. Qin and T. Wang contributed equally to this article.

Note: Supplementary data for this article are available at Cancer Research Online (http://cancerres.aacrjournals.org/).

Corresponding Authors: Bin Wang and Dong-feng Chen, Department of Gastroenterology, Daping Hospital, Army Medical University (Third Military Medical University), Gaotanyan 30, Shapingba District, Chongqing 400038, China. Phone: 86-023-68757741; Fax: 86-023-68757741; E-mail: wb_tmmu@126.com; chendf1981@126.com

Cancer Res 2019;79:4869–81

doi: 10.1158/0008-5472.CAN-19-0442

Introduction

Aberrant epigenetic modifications are essential hallmarks of human cancers. Such alterations disrupt homeostatic epigenetic status and allow cells to override physiologic differentiation and growth control (1). In this regard, histone lysine acetylation is frequently deregulated in cancer, in part due to expression and activity changes in histone acetyltransferases and/or histone deacetylases (HDAC; ref. 2). Acetylated lysine residues serve as docking sites for reader proteins that harbor bromodomain(s), including the bromodomain and extraterminal domain (BET) proteins (BRD2, BRD3, BRD4, and testis-specific BRDt; ref. 3). BET proteins have two conserved bromodomains that recognize acetylated histones and act as scaffolds to recruit transcriptional coactivators to promoters and superenhancers, therefore driving gene transcription and cancer growth (3). Bromodomains also recognize acetylated lysines on nonhistone proteins such as RelA (3); however, the biological functions of BRD4 recognition of nonhistone proteins remain largely unclear.

Unbiased genetic screens in a variety of cancers have revealed that genes encoding BET proteins, especially BRD4, are essential for cell survival and also are promising anticancer targets (4, 5). To date, there are more than 30 ongoing clinic trails in evaluating therapeutic efficacy of BET inhibitors in a series of malignancies (6). Although extensively pursued in clinical investigations, detailed pathophysiologic functions of BET proteins are less understood. Homozygous deletion of BRD2 or BRD4 leads to embryonic lethality (7, 8), highlighting their fundamental roles in embryogenesis. Although BET proteins are seemingly general transcriptional regulators, BET inhibition only affects a subset of lineage-specific genes (3, 9). Thus, the functions of BET proteins appear to be highly context-dependent and are still poorly understood in various developmental and disease conditions.

Several transcription factors including Snail family transcriptional repressor 1 (Snail) are known as important regulators of tumor invasion and metastasis (10). Recent genetic studies in mice have demonstrated that Snail also plays an important role in tumor initiation and progression (11, 12). As a key regulator of tumorigenesis, the abundance of Snail is tightly controlled by ubiquitination and rapid proteasomal degradation in cells (13–15). Snail ubiquitination is established by several E3 ubiquitin ligase complexes including SCF (Skp1-Cullin1-F-box)-β-TrCP1, SCF-FBXO11 and SCF-FBXL14 (13–15), and removed by deubiquitinase 3 (16, 17). Interestingly, Snail acetylation by acetyltransferase CREB-binding protein (CBP) has been reported to stabilize Snail (18), whereas the underlying molecular mechanism remains unknown.

In the present study, we identified an essential role of the epigenetic regulator BRD4 in maintaining gastric cancer progression and metastasis. Mechanistically, BRD4 interacts with Snail in an acetylation-dependent manner, thereby preventing FBXL14 and β-Trcp1 binding to and degradation of Snail. Our results suggest that the BRD4–Snail signaling axis deserves further explorations to develop targeted therapies in treating metastatic gastric cancer in clinic.

Materials and Methods

Reagents and antibodies

Chemical reagents including MG132, bafilomycin A1, and bromodomain inhibitor JQ1, OTX-101, were purchased from Selleckchem. Cycloheximide and actinomycin D were obtained from R&D Systems. Anti-BRD4 antibodies were from Cell Signaling Technology, Abcam, and Bethyl. Anti-BRD2 and anti-BRD3 antibodies were purchased from Abcam. Anti-Snail antibodies were obtained from Cell Signaling Technology, Santa Cruz Biotechnology, and Proteintech. Epithelial–mesenchymal transition antibody sampler kit (including Slug, ZO-1 TCF8/ZEB1), anti–GSK-3β, anti–phospho-GSK-3β (Ser9), and anti–acetylated-lysine antibodies were purchased from Cell Signaling Technology. Anti-Twist antibody was from Santa Cruz Biotechnology. Normal mouse IgG and rabbit IgG antibodies were from Beyotime. As for Tag antibodies, rabbit polyclonal anti-Flag antibody was obtained from Proteintech, whereas mouse monoclonal anti-Flag antibody was from Origene. Rabbit polyclonal Anti-GFP antibody was from Novus, whereas mouse monoclonal anti-GFP antibody was from Proteintech. Rabbit monoclonal anti-HA antibody was from Cell Signaling Technology, whereas mouse monoclonal anti-HA antibody was from Origene. Anti-His antibody was purchased from Proteintech. Detailed information about antibody usage was described in Supplementary Table S1.

Patient specimens and IHC staining

Paraffin-embedded gastric cancer tissue was obtained from individual patients with written-informed consent and with approval by the Institutional Review Board. Gastric cancer tissues and adjacent mucosa were collected from patients who were diagnosed as gastric cancer at the department of general surgery in Daping Hospital. Tissue sections (4 μm) were subjected to standard protocols for deparaffinization and were rehydrated in graded ethanol. Antigens were retrieved by 10 mmol/L sodium citrate (for BRD4) or EDTA (for Snail), respectively. Tissues were blocked by goat serum for 30 minutes at 37°C and then incubated with primary antibody overnight at 4°C (BRD4, Bethyl 1:8,000; Snail, Proteintech 1:200; β-TRCP1, GeneTex 1:400; FBXL14, Proteintech 1:100). After washing with PBS 3 times, tissue sections were incubated with horseradish peroxidase (HRP)–conjugated secondary antibody (DAKO) at 37°C for 30 minutes. Then sections were visualized by DAB (DAKO) and counterstained by hematoxylin. Images were captured on an Olympus BX51 microscope. We followed a previously described protocol to quantify staining intensity (19). Five representative fields of a section were evaluated by two double-blinded pathologists. Final score of BRD4 and Snail in each sample was obtained by multiplying the strength score by the distribution score. The cutoff score in various analyses was 8 for both anti-BRD4 and anti-Snail staining intensity (high expression, IHC scoring $\geq$ 8; low expression, IHC scoring < 8).

Constructs, siRNAs, lentivirus, and CRISPR-Cas9–mediated gene knockout

Constructs for GFP-BRD2, GFP-BRD3, GFP-BRD4, and His-ub were purchased from Addgene. Flag-Snail vector was purchased from Origene to generate Flag-Snail-K146R (lysine to arginine mutation) and Flag-Snail-K146R and Flag-Snail-KRKR (K146R, K187R). HA-FBXL14 and HA-β-Trcp1 constructs, as well as siRNAs targeting BRD2, BRD3, and BRD4 were purchased from Sangon Biotech. Lipofectamine 3000 Transfection Reagent (Invitrogen) was used for plasmids and siRNAs transfection.

For stable expression of MYC in gastric cancer cells, lentivirus-packaging procedures were performed as previously described (20). MYC cDNA was a kind gift from Professor Jiang Jun (Urinary Surgery of Daping Hospital), and Snail cDNA was purchased from Origene.

To generate *BRD4* or *Snail* knockout cell lines, CRISPR-Cas9 gene editing technology was utilized as reported (21). Three independent sgRNAs targeting BRD4 and Snail were designed using the online tool from Zhang lab (http://crispr.mit.edu; sgBRD4-1: CACCGACAGGAGGAGGATTCGGCTG; sgBRD4-2: CACCGGTCGATGCTTGAGTTGTGTT; sgBRD4-3: CACCGGGGAACAATAAAGAAGC GCT; sgSnail-1: CACCGTCCTGCAGCTCGCTGTAGTT; sgSnail-2: CACCGACTCTCCTGGAGCCG AAGGG; sgSnail-3: GGTTGAGGATCTCCGGAGGT). The sgRNAs were incorporated into the pLentiCRISPR v2 (Addgene plasmid # 52961) construct to generate lentivirus. After transfection, single-cell isolation, and expansion, *BRD4* and *Snail* knockout and control cell lines were obtained and confirmed using both genome sequencing and Western blot analysis.

Immunoblot and immunoprecipitation

Whole-cell lysates were extracted by RIPA Lysis and Extraction Buffer (Thermo Scientific) containing protease and phosphatase inhibitor (BD Biosciences). Protein concentration was measured by Enhanced BCA Protein Assay Kit (Beyotime). A total of 30 μg of protein were separated in 10% SDS-PAGE and transferred into the polyvinylidene difluoride membranes (0.44 μm, Millipore). Membranes were blocked in 5% skim milk [dissolved in PBS with 0.1% tween-20 (PBST)] and incubated with indicated primary antibodies at 4°C overnight. After extensive washing with PBST, the membranes were incubated with proper HRP-labeled goat secondary antibody (Santa Cruz Biotechnology). The chemical signal was visualized by SuperSignal West Femto Maximum Sensitivity Substrate (Thermo Scientific). The images were taken on a ChemiDoc imaging System (Bio-Rad) and analyzed by Image Lab software.

For immunoprecipitation, all protocols followed instructions of Pierce Classic Magnetic IP/Co-IP Kit (Thermo Scientific). In brief, fresh cell lysates were incubated with indicated primary antibodies (2–4 μg) in a BeyoMagMagnetic Separation Rack (Beyotime) at 4°C for 6 hours. Then, the Pierce Protein A/G Magnetic Beads (Thermo Scientific) were added and incubated for 1 hour. After washing with PBST, the immunoprecipitates were eluted, neutralized, and SDS degenerated for further immunoblot.

Protein half-life assay

To estimate the half-life of Snail protein in different conditions, cycloheximide pulse-chase experiments were performed as previously described (22). In brief, cells were seeded in 6-well plate, and cycloheximide was added in the media at indicated time points. Whole-cell lysates were collected for immunoblot.

Ubiquitination assay

To detect Snail ubiquitination, nickel-nitrilotriacetic acid (Ni-NTA) pull-down assay was performed (22). In brief, 293T cells were transfected with His-Ub (ubiquitin) and indicated vectors, pretreated with MG132 for 8 hours. Whole-cell lysates were collected using by Buffer A [6 mol/L guanidine-Hcl, 0.1 mol/L Na_2HPO_4/NaH_2PO_4, 10 mmol/L imidazole (pH 8.0) for 250 mL]. After ultrasonication and centrifugation, lysates were purified using Ni-NTA (QIAGEN) for 3 hours at room temperature. Purification products were washed in each Buffer A, Buffer A/Buffer TI (1:3), and Buffer TI (25 mmol/L Tris-CL, 20 mmol/L imidazole). The pull-down products were then separated by SDS-PAGE for immunoblot analysis.

All animal experiments were approved by the Institutional Animal Care and Use Committee of the Army Medical University. RNA sequencing data were deposited to the NCBI database under accession number GSE134150. For additional Materials and Methods, please refer to the Supplementary Materials.

Results

High levels of BRD4 expression in human gastric cancer tissues are associated with distal metastasis and poor clinical outcomes

To examine the potential roles of BET subfamily members in gastric cancer, we analyzed RNA-sequencing results from The Cancer Genome Atlas (TCGA) and GTEx database. We found that, compared with adjacent normal epithelia, the mRNA levels of BRD4 but not BRD2 nor BRD3 were elevated in gastric cancer and several other gastrointestinal malignancies (Fig. 1A and Supplementary Fig. S1A–S1C). Using two independent datasets, we demonstrated that high expression of BRD4 transcripts in gastric cancer tissues was associated with shorter overall survival and progression-free survival in patients (Fig. 1B and Supplementary Fig. S1D–S1I). These results suggest that BRD4 may play an important role in gastric cancer progression.

BRD4 expression was further validated using an in-house gastric cancer cohort by IHC. Compared with matched normal gastric mucosa, BRD4 protein expression was significantly higher in cancerous tissues (Fig. 1C and D). Elevated expression of BRD4 was correlated with clinicopathologic parameters such as older age ($\geq$60), tumor location, and advanced clinical stage (Supplementary Table S2). Semiquantitative analyses revealed that gastric cancer tissues with lymph node metastasis (N1+N2+N3) showed increased BRD4 staining compared with those without lymph node metastasis (Fig. 1D), indicating potential involvement of BRD4 in tumor cell dissemination. Consistent with this notion, analyzing follow-up data demonstrated that gastric cancer patients with distal metastasis later displayed higher levels of BRD4 expression in their primary tumors (Fig. 1E and F). Moreover, compared with patients with BRD4-low tumors, those with BRD4-high tumors showed shorter overall survival and were more likely to develop metastatic lesions (Fig. 1G and H). Together, elevated expression of BRD4 in gastric cancer may contribute to metastasis of gastric cancer cells in patients.

BRD4 maintains invasion and dissemination of cancer cells through a mechanism that is independent of its characterized transcriptional targets MYC and BCL2

We next sought to understand how BRD4 contributes to malignancy of gastric cancer. Depleting *BRD4* or inhibiting BRD4 activity using JQ1 decreased cell growth and tumorigenicity, which was restored by reintroducing MYC in gastric cancer cells (Fig. 2A and Supplementary Fig. S2A–S2I). In light of the significant association between BRD4 abundance and cancer metastasis, we further assessed the role of BRD4 in cell motility and invasiveness, two initiation steps of cancer cell metastasis. We

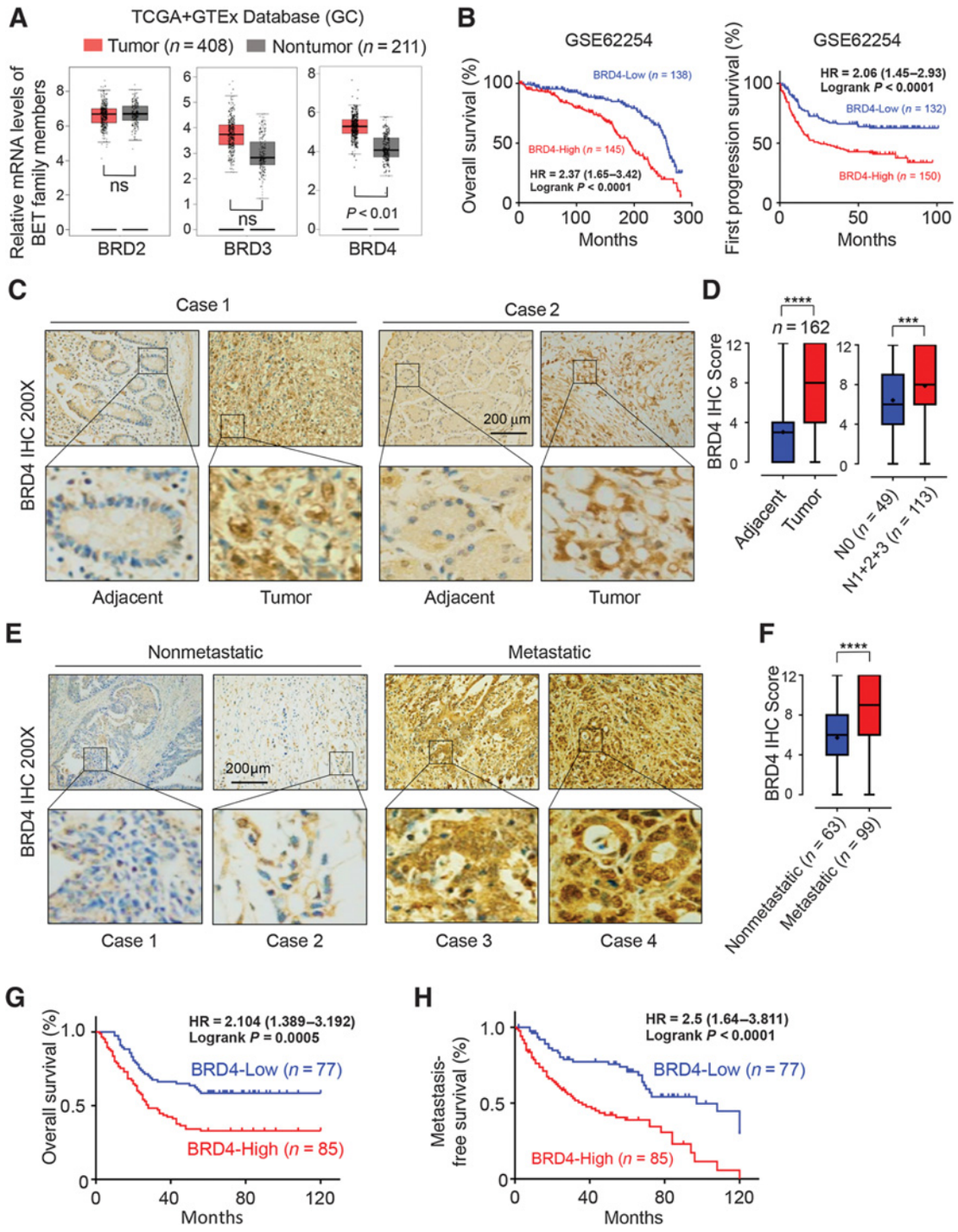

Figure 1.

High expression of BRD4 in human gastric cancer tissues is associated with cancer metastasis. **A,** Gene Expression Profiling Interactive Analysis data from the TCGA and GTEx databases demonstrated elevated mRNA level of BRD4, but neither BRD2 nor BRD3 in gastric cancer (GC) compared with nontumor tissue (red box, tumor tissues; gray box, nontumor tissues). **B,** Kaplan–Meier survival analysis using KM plotter (dataset—226054) indicated that upregulation of BRD4 mRNA levels in gastric cancer was associated with decreased probabilities of overall survival (left plot) and first progression survival (right plot) in patients. **C** and **E,** Representative IHC images of gastric cancer and adjacent gastric epithelial tissues (**C**), or in gastric cancer tissues with or without distal metastasis (**E**). **D** and **F,** The staining intensity of BRD4 was quantified and is presented as mean ± SD ($n = 162$). ***, $P < 0.001$; ****, $P < 0.0001$. **G** and **H,** Kaplan–Meier survival analysis showed that elevated expression of BRD4 in gastric cancer tissues correlates with shortened overall survival (**G**) and metastasis-free survival (**H**) of patients.

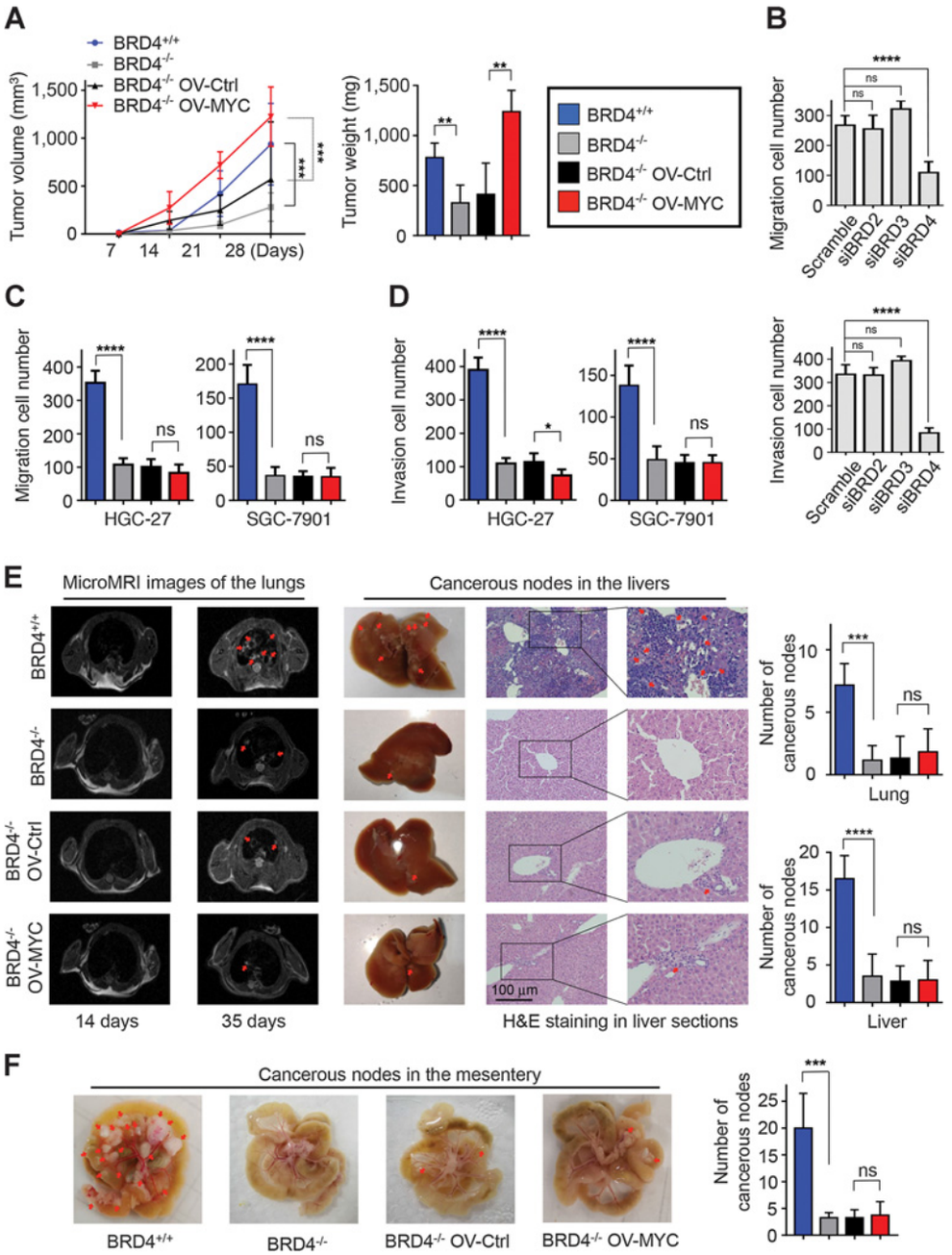

Figure 2.

Depleting *BRD4* attenuates invasiveness and metastasis of gastric cancer cells, a phenotype that does not rely on its putative transcriptional targets MYC. **A,** Reintroducing MYC restores tumor growth of *BRD4*-depleted gastric cancer cells. *BRD4*$^{-/-}$ HGC-27 cells infected with control (OV-Ctrl) or MYC-expressing (OV-MYC) lentivirus were inoculated subcutaneously into the left flank of nude mice. The growth kinetics (left) and weight (right) of the xenografts are presented as mean ± SD ($n = 5$ for each group). The dissected xenograft tumors are shown in Supplementary Fig. S2F. **B,** Depletion of *BRD4* inhibits migration and invasion of HGC-27 cells. Transwell migration (top) and invasion (bottom) assay using cells transfected with siRNAs targeting scramble, BRD2, BRD3, and BRD4. Representative images are shown in Supplementary Fig. S3B. **C** and **D,** Reintroducing MYC fails to enhance migration and invasion of *BRD4*-depleted gastric cancer cells. Transwell migration (**C**) and invasion (**D**) assays using wild-type HGC-27 and SGC-7901 cells, or *BRD4*-depleted cells infected with indicated lentivirus. Representative images are shown in Supplementary Fig. S3C. **E,** Reintroducing MYC does not recover metastatic capacity of *BRD4*-depleted cells. Representative MRI lung images of NOD-SCID mice injected via tail vein with indicated gastric cancer cells on 14 and 35 day (left). Hematoxylin and eosin (H&E) staining images of metastatic lesions in the livers of these mice are also shown (middle). Right, quantitative data of lung and liver metastases are shown ($n = 5$ mice per group). **F,** Representative images (left) and quantitative data of peritoneal metastatic foci formed by indicated HGC-27 cells (right; $n = 5$ mice per group). Hematoxylin and eosin–stained images of foci are shown in Supplementary Fig. S3G. Results were validated by three biological repeat experiments. Representative images are presented (**E** and **F**), and data are presented as the mean ± SD (**A**–**F**). ns, no significance. *, $P < 0.05$; **, $P < 0.01$; ***, $P < 0.001$; ****, $P < 0.0001$.

found that depletion of *BRD*4, but not *BRD2* and *BRD3*, by siRNA, potently inhibited cell migration and invasion, suggesting that BRD4 might be selectively required for dissemination of gastric cancer cells (Fig. 2B and Supplementary Fig. S3A and S3B). Moreover, depleting *BRD4* or inhibiting BRD4 activity suppressed cell migration and invasion, whereas ectopic expression of BRD4 enhanced cell motility and invasiveness (Fig. 2C and Supplementary Fig. S3C–S3F). These results indicate that the growth-promoting BRD4 may also function as a regulator of cancer cell metastasis.

BRD4 is known to promote cell growth in part through targeting MYC and BCL2 in hematopoietic malignancies (3, 5). However, reintroducing MYC or BCL2 in *BRD4*-depleted cells could not restore impaired cell motility and invasiveness (Fig. 2C and D and Supplementary Fig. S3C). To avoid potential artifacts of our *in vitro* assays, we developed two independent metastasis models in NOD-SCID mice. In a lung and liver metastasis model, a MicroMRI system was applied to detect the metastatic lesions in the lungs following injection of cancer cells via tail vein. We found that loss of *BRD4* in gastric cancer cells led to fewer pulmonary cancerous nodes, which could not be rescued by lentiviral delivery of MYC (Fig. 2E, left). Hematoxylin and eosin staining of liver tissue sections revealed that depletion of *BRD4* abrogated the formation of micrometastases in the liver, which could not be restored by MYC overexpression (Fig. 2E, middle). Moreover, in a peritoneal metastasis model, reintroducing BRD4 transactional target MYC (Fig. 2F and Supplementary Fig. S3G) also failed to restore impaired colonizing capacity of $BRD4^{-/-}$ cells in the mesentery. These data suggest that BRD4 may promote gastric cancer metastasis in a manner independent of its known transcriptional targets MYC or BCL2.

BRD4 stabilizes Snail proteins by preventing its proteasomal degradation

Given that several epithelial-to-mesenchymal-transition–inducing transcription factors are key regulators of tumor metastasis (10), we examined whether their expression levels were regulated by BRD4. Ectopic expression of BRD4 increased protein levels of Snail, but not Slug, Twist, or Zeb1, in a dose-dependent manner (Fig. 3A and Supplementary Fig. S4A). Conversely, depleting endogenous *BRD4* or inhibiting BRD4 activity by JQ1 significantly downregulated Snail protein levels (Fig. 3B and Supplementary Fig. S4B and S4C). On the other hand, manipulation of BRD2 and BRD3 failed to significantly and consistently regulate Snail protein levels (Supplementary Fig. S4D and S4E). Intriguingly, unlike the well-established BRD4 transcriptional target MYC, Notch1, and IL15RA (23), Snail mRNA levels were minimally affected by manipulating BRD4 expression or activity (Fig. 3C and D and Supplementary Fig. S4C and S4F–S4I). Consistent with this notion, inhibition of mRNA transcription or translation by Actinomycin D and Cycloheximide, respectively, failed to reduce Snail protein levels (Supplementary Fig. S4J), indicating that BRD4 may control Snail expression at the post-translational levels.

The Snail protein has a short half-life through constant ubiquitin–proteasome-mediated protein degradation (13–15). Therefore, we tested whether BRD4 controls Snail protein stability in cells. In this regard, Snail protein levels were rescued by blocking proteasome activity using MG132 in cells depleted of *BRD4* or treated with JQ1 (Supplementary Fig. S4K, S4L), but not in cells treated with the lysosome inhibitor Bafilomycin A. These data suggest that BRD4 positively regulates Snail protein stability through inhibiting its proteasome-dependent degradation. Consistently, cycloheximide pulse-chase assays showed that ectopic expression of BRD4 extended, while depleting endogenous *BRD4* shortened, the half-life of the Snail proteins in cells (Fig. 3E and Supplementary Fig. S4M). Therefore, BRD4 stabilizes Snail proteins by preventing its proteasomal degradation.

BRD4 interacts with Snail and interferes with E3 ligases–governed Snail ubiquitination

Immunofluorescence staining revealed that BRD4 colocalized with Snail in gastric cancer cells, indicating that BRD4 may interact with Snail (Supplementary Fig. S4N), which was confirmed by immunoprecipitation assays (Fig. 3F). Furthermore, JQ1 treatment leads to attenuated BRD4 binding to Snail, supporting a critical role of acetylation in mediating this interaction (Fig. 3G). Interestingly, unlike BRD4, both BRD2 and BRD3 displayed minimal binding to Snail at endogenous levels (Supplementary Fig. S4O). Previously, BRD4 was reported to interact with Twist to promote tumorigenesis in basal-like breast cancer (18), whereas in gastric cancer cells, Snail but not Twist was the major BRD4-binding partner (Supplementary Fig. S4P). Therefore, BRD4 may drive gastric cancer metastasis primarily through binding Snail to regulate its function.

We next examined whether BRD4 engagement affected Snail ubiquitination, thereby regulating its protein stability. We observed that depletion of *BRD4* increased, whereas ectopic expression of BRD4 suppressed, polyubiquitination of Snail (Fig. 3H and I). BRD4-binding–mediated inhibition of Snail polyubiquitination was also mitigated by JQ1 (Fig. 3J), suggesting that BRD4 may suppress Snail polyubiquitination in a BRD4-bromodomain and Snail acetylation–dependent manner. Previous studies have demonstrated that activated GSK-3β phosphorylates and primes Snail for its E3 ligase–mediated ubiquitination; however, GSK-3β activity remained unchanged upon JQ1 treatment (Supplementary Fig. S4Q). These observations suggest that BRD4 may not directly inhibit E3 ligases regulating Snail, but rather impeding access of Snail to its physiologic E3 ligases.

BRD4 recognizes Snail in an acetylation-dependent manner

BRD4 recognizes acetylated lysine residues on histone tails via its bromodomain to exert epigenetic regulatory functions (3). Moreover, Snail has been reported to be acetylated by the acetyltransferase CBP and deacetylated by HDAC family members (18). Our observation that JQ1 treatment reduced BRD4 binding to Snail (Fig. 3G) led us to hypothesize that BRD4 might recognize acetylated Snail through its bromodomain. Consistently, inhibiting HDAC activity by trichostatin A or ectopic expression of CBP to enhance Snail acetylation led to enhanced binding of BRD4 with Snail (Fig. 4A and B). Notably, CBP upregulated the protein levels of Snail in a BRD4-dependent manner (Fig. 4C).

There are two reported evolutionally conserved lysine residues in Snail that are acetylated (K146, K187; Fig. 4D; ref. 18). Mutating either or both of them significantly reduced the levels of Snail acetylation and subsequently abolished the interaction between BRD4 and Snail (Fig. 4D). These observations support that BRD4 interacts with Snail in a Snail acetylation–dependent manner. As a result, BRD4 prolonged half-life of wild-type but not acetylation-

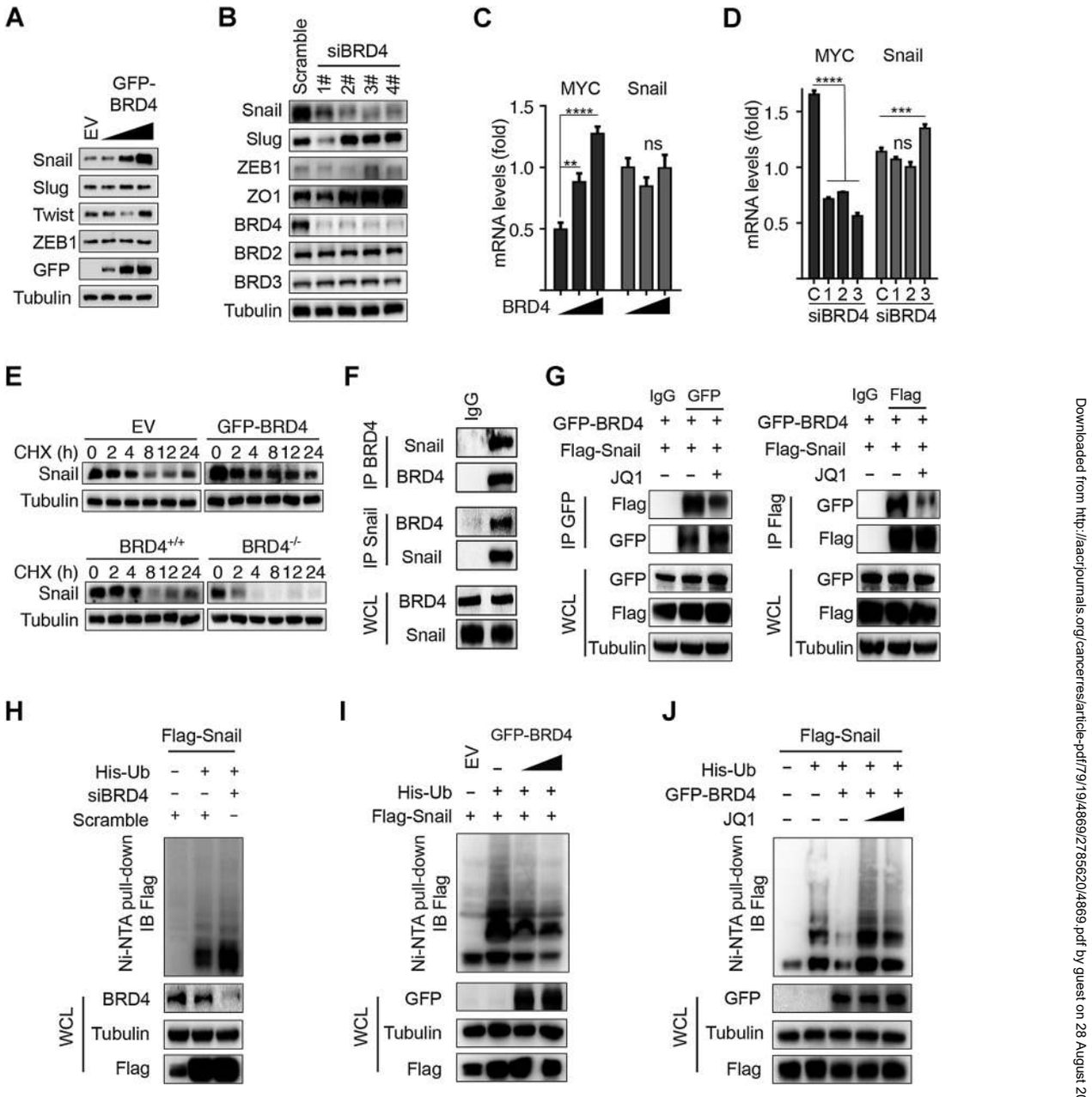

Figure 3.

BRD4 stabilizes Snail protein by inhibiting its ubiquitination. **A,** Immunoblot analysis of the abundance of core metastasis-related transcription factors in HGC-27 cells transfected with increasing amount of BRD2, BRD3, or BRD4 expression constructs. **B,** HGC-27 cells transfected with BRD4-targeting siRNAs for 48 hours. Whole-cell lysates (WCL) were collected for Western blot analysis with indicated antibodies. **C** and **D,** HGC-27 cells transfected with BRD4-expressing plasmid (**C**) or BRD4-specific siRNAs (**D**). Total RNA was collected for qPCR analysis. **E,** BRD4 promotes stability of endogenous Snail protein. HGC-27 cells transfected with GFP-BRD4 or empty constructs (top), or $BRD4^{+/+}$ or $BRD4^{-/-}$ cells (bottom) were treated with cycloheximide (CHX) for indicated time course. Whole-cell lysates were collected for immunoblot analysis. Snail immunostaining intensity was quantified and is shown in Supplementary Fig. S4M. **F,** BRD4 interacts with Snail at endogenous levels. Western blot analysis of whole-cell lysates, anti-Snail, or anti-BRD4 immunoprecipitates of HGC-27 cells. Normal IgG was included as a negative control. **G,** HEK-293T cells cotransfected with GFP-tagged BRD4 and Flag-tagged Snail constructs were treated with JQ1 or DMSO. Whole-cell lysates, anti-GFP (left), or anti-Flag (right) immunoprecipitates were immunoblotted with indicated antibodies. **H,** Depleting *BRD4* increases the ubiquitination of Snail. HEK-293T cells transfected with indicated constructs together with scramble or BRD4-specific siRNA and then treated with MG132 (20 μmol for 8 hours). Ni-NTA pull-downs and whole-cell lysates were subject to immunoblot analysis. **I** and **J,** Ectopic expression of BRD4 suppresses the ubiquitination of Snail, which was reversible by JQ1 treatment. HEK-293T cells transfected with indicated constructs or empty vector (EV) as a control (**I**), or further treated with JQ1 (**J**). Following incubation with MG132 (20 μmol) for 8 hours, Ni-NTA pull-downs and whole-cell lysates were prepared for immunoblot analysis. Results were validated by three separate experiments. Tubulin was used as a loading control. Representative images are presented (**A**, **B**, and **E**–**J**) and data are presented as the mean ± SD (**C** and **D**). ns, no significance. **, $P < 0.01$; ***, $P < 0.001$; ****, $P < 0.0001$.

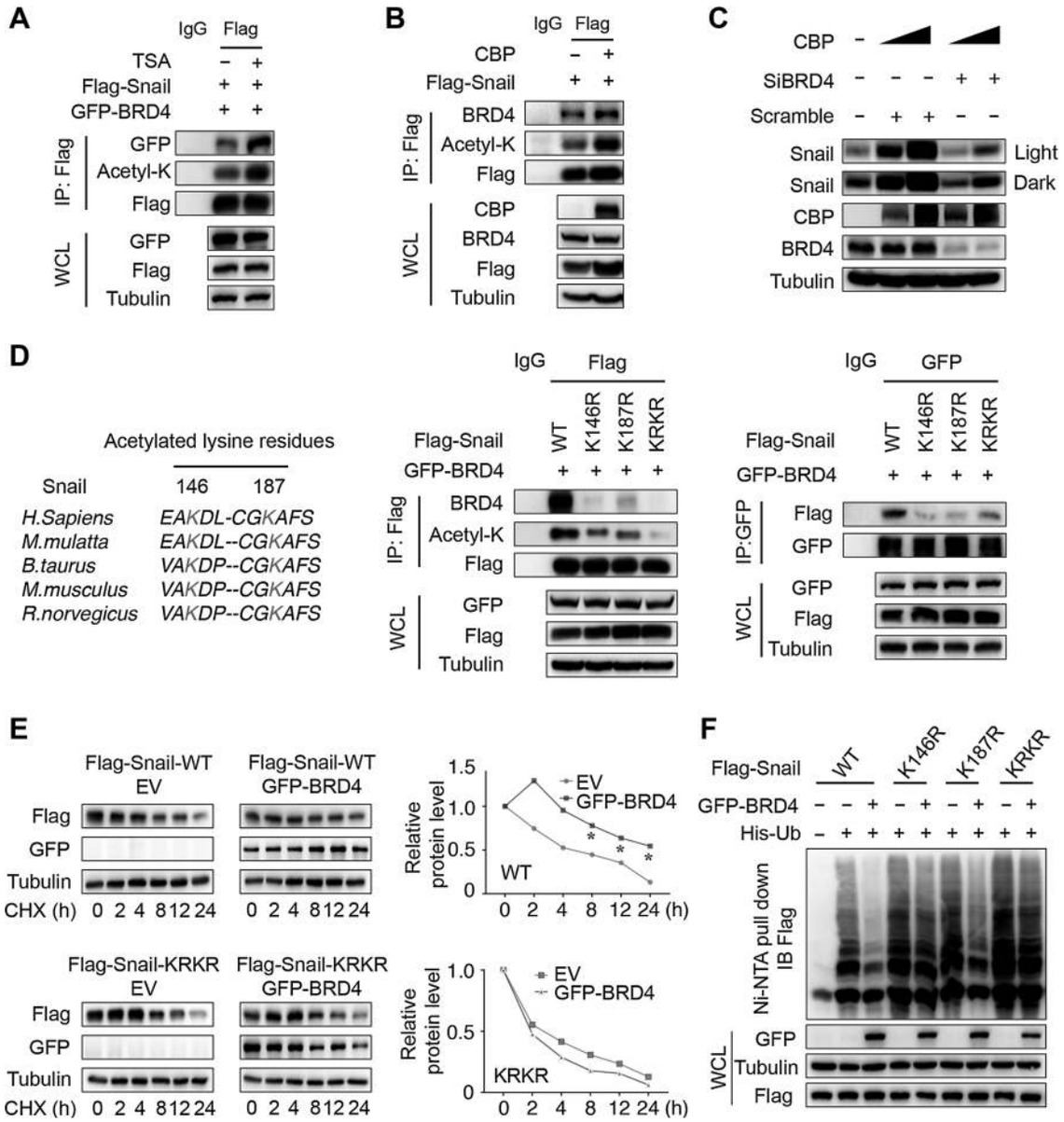

Figure 4.

BRD4 interacts with Snail to restrain its degradation in an acetylation-dependent manner. **A** and **B,** Acetylation of Snail enhances its interaction with BRD4. HEK-293T cells transfected indicated constructs in the presence (**A**) or absence (**B**) of trichostatin A (TSA), followed by incubation with MG132 for 8 hours. Anti-Flag immunoprecipitates and whole-cell lysates (WCL) were collected for immunoblot analysis. **C,** HEK-293T cells transfected with scramble or BRD4-specific siRNAs, together with CBP constructs for 48 hours. Whole-cell lysates were collected for immunoblot analysis. **D,** Acetylation of Snail is required for its interaction with BRD4. The two Snail acetylation residues, K146 and K187, were evolutionally conserved (left). HEK-293T cells transfected with GFP-tagged BRD4 construct, together with different Flag-tagged Snail vectors (WT, wild-type; K146R; K187R; and KRKR). Anti-Flag (middle) or anti-GFP (right) immunoprecipitates and whole-cell lysates were collected for immunoblot analysis. **E,** BRD4 stabilizes wild-type, but not acetylation-deficient, Snail in cells. HEK-293T cells transfected with GFP-tagged BRD4 or GFP alone constructs, or together with Flag-tagged wild-type or acetylation-deficient Snail (Snail-WT or Snail-KRKR). Cells were then treated with cycloheximide (CHX) for indicated time course. Whole-cell lysates were collected for immunoblot analysis, and staining intensity was quantified to present as mean ± SD. **F,** BRD4 inhibits the ubiquitination of wild-type but not acetylation-deficient Snail. HEK-293T cells transfected with indicated constructs in the presence of JQ1. Following incubation with MG132 (20 μmol) for 8 hours, Ni-NTA pull-downs and whole-cell lysates were prepared for immunoblot analysis. *, $P < 0.05$.

deficient mutated forms of Snail in cells (Fig. 4E and Supplementary Fig. S5A) largely through BRD4-mediated suppression of ubiquitination of wild-type, but not acetylation-deficient mutated forms of Snail (Fig. 4F). These results suggest that BRD4 recognizes acetylated Snail in cells, thereby stabilizing Snail by suppressing its ubiquitination.

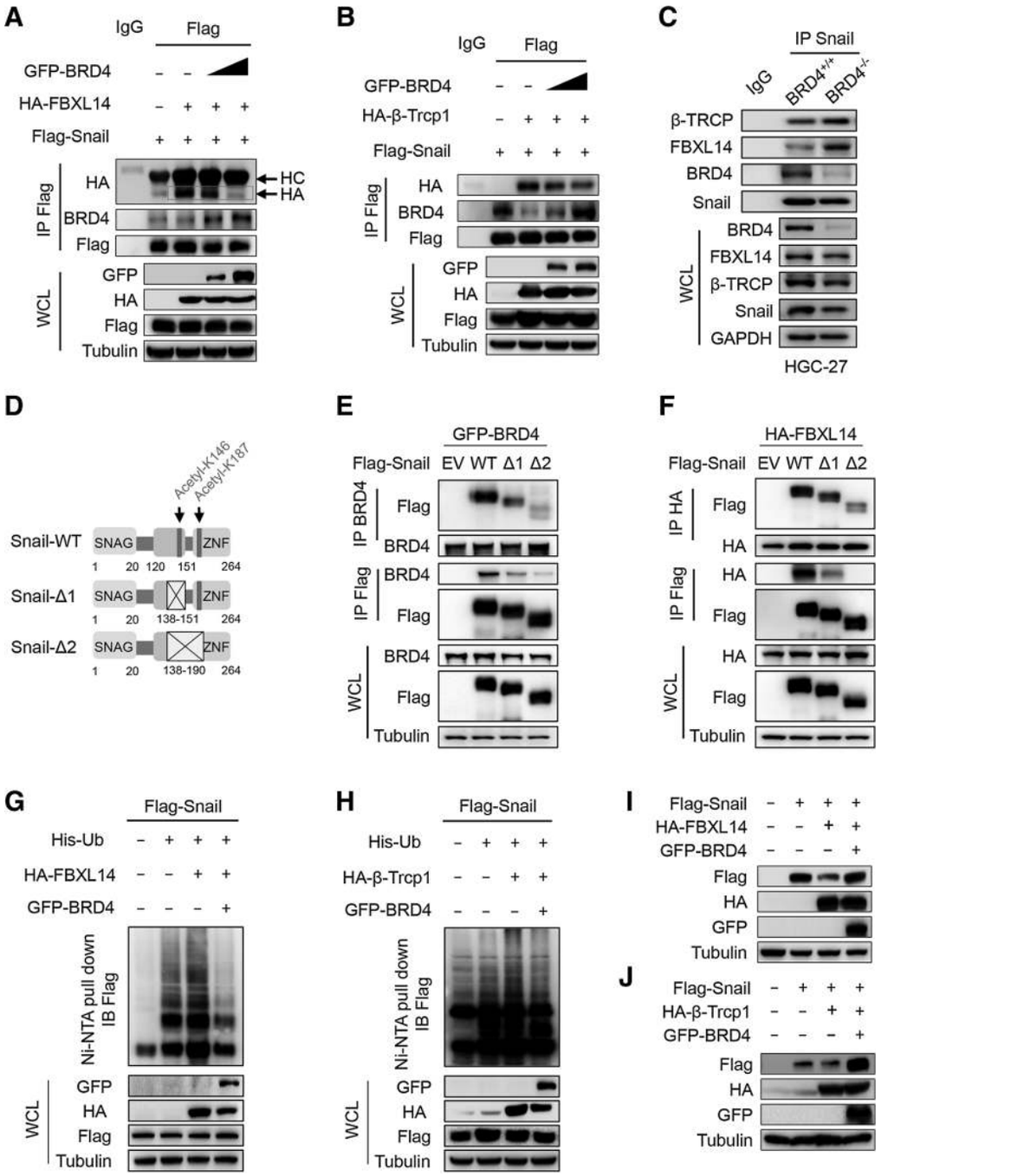

Figure 5.

BRD4 decreases the ubiquitination of Snail by occluding the E3 ligases FBXL14 and β-Trcp1. **A** and **B,** BRD4 competes with FBXL14 and β-Trcp1 for binding Snail. HEK-293T cells transfected with Flag-Snail and GFP-BRD4, together with hemagglutinin (HA)-tagged FBXL14 (**A**) or β-Trcp1 constructs (**B**), and then incubated with MG132 for 8 hours. Whole-cell lysates (WCL) and anti-Flag immunoprecipitates were detected by immunoblot analysis. **C,** BRD4 competes with FBXL14 and β-Trcp1 for binding Snail at endogenous levels. BRD4$^{+/+}$ and BRD4$^{-/-}$ HGC-27 cells incubated with MG132 for 8 hours. Whole-cell lysates and anti-Snail immunoprecipitates were detected by immunoblot analysis. **D**–**F,** BRD4 and FBXL14 occupy a similar domain in Snail. Schematic model of the domain structure of wild-type Snail (Snail-WT) and Snail mutants depleting either aa138-151 (Snail-Δ1) or aa138-190 (Snail-Δ2; **D**). HEK-293T cells transfected with indicated Snail mutants, together with either GFP-BRD4 (**E**) or HA-FBXL14 (**F**) for 48 hours. Whole-cell lysates and immunoprecipitates were detected by immunoblot analysis. **G** and **H,** BRD4 competes with FBXL14 and β-Trcp1 to inhibit the ubiquitination of Snail. HEK-293T cells transfected with Flag-Snail and His-Ub, together with HA-tagged FBXL14 (**G**) or β-Trcp1 constructs (**H**), in the presence or absence of GFP-BRD4. The cells were incubated with MG132 for 8 hours, and Ni-NTA pull-downs and whole-cell lysates were prepared for immunoblot analysis. **I** and **J,** BRD4 antagonizes FBXL14 and β-Trcp1–mediated degradation of Snail. HEK-293T cells transfected with Flag-Snail and HA-FBXL14 (**I**) or β-Trcp1 constructs (**J**) in the presence or absence of GFP-BRD4. Whole-cell lysates were prepared for immunoblot analysis.

BRD4 competes with the E3 ligases FBXL14 and β-Trcp1 to bind Snail, thereby decreasing Snail ubiquitination

We next sought to understand mechanistically how interaction between BRD4 and Snail suppresses Snail ubiquitination and degradation. To this end, several E3 ubiquitin ligases have been reported to promote Snail ubiquitination, including FBXL14, β-Trcp1, and FBXO11 (13–15). Ectopic expression of BRD4 decreased Snail binding to either FBXL14 or β-Trcp1 in a dose-dependent manner (Fig. 5A and B). On the other hand, ectopic expression of either FBXL14 or β-Trcp1 also suppressed Snail binding to BRD4 (Supplementary Fig. S6A and S6B). Importantly, depleting *BRD4* in gastric cancer cells enhanced the interaction between Snail and its E3 ubiquitin ligases including FBXL14 and β-Trcp1 at endogenous levels (Fig. 5C). This mutually exclusive binding pattern with BRD4 for Snail was not observed with another reported Snail E3 ubiquitin ligase FBXO11. In addition, the acetylation-deficient Snail mutant exhibited elevated binding to both FBXL14 and β-Trcp1 (Supplementary Fig. S6C and S6D), supporting that Snail acetylation may serve as a key modification to regulate is interaction with either BRD4 or Snail E3 ligases.

Next, we explored how BRD4 blocked FBXL14 and β-Trcp1 binding to Snail. FBXL14 interacted with Snail through a Snail domain containing the acetylation residues (K146 and K187; ref. 14). We generated two Snail truncation mutations lacking these residues (Snail-Δ1 and Snail-Δ2) and found that FBXL14 and BRD4 recognized the same Snail K146/K187 acetylation-containing motif (Fig. 5D–F). Thus, BRD4 binding to Snail may render Snail less accessible for FBXL14. On the other hand, β-Trcp1 recognizes a "DSGxxS" degron in Snail that is phosphorylated by GSK-3β to mediate Snail ubiquitination and subsequent proteasomal degradation (24). We found that BRD4 Bromodomains that bind Snail significantly attenuated GSK-3β–mediated Snail phosphorylation *in vitro* (Supplementary Fig. S6E). Thus, BRD4 may restrain β-Trcp1 binding to Snail through suppressing GSK-3β–mediated priming Snail phosphorylation events.

Consistent with these observations, ectopic expression of BRD4 partially mitigated ubiquitination of Snail mediated by either FBXL14 or β-Trcp1 (Fig. 5G and H) and led to Snail resistance to FBXL14- or β-Trcp1–mediated degradation (Fig. 5I and J). These observations suggest that BRD4 forms a complex with Snail in an acetylation-dependent manner in cells, which protects Snail from FBXL14- or β-Trcp1–mediated ubiquitination and proteasomal degradation.

Snail is necessary and sufficient in driving BRD4-associated cancer metastasis

We next assessed cellular functions of BRD4-mediated stabilization of Snail. Lentiviral delivery of Snail in $BRD4^{-/-}$ cells significantly restored cell migration and invasion, leading to enhanced peritoneal dissemination *in vivo* (Fig. 6A and B; and Supplementary Fig. S7A and S7B), suggesting that Snail is the major downstream target through which BRD4 promotes cell metastasis. However, BRD4 could not rescue impaired cell migration and invasion caused by *Snail* depletion (Supplementary Fig. S7C and S7D), demonstrating that Snail is necessary for BRD4 to promote cell invasion. Although Snail is the major BRD4 target in regulating cell migration, ectopic expression of Snail in $BRD4^{-/-}$ cells only minimally rescued cell growth defects in clone formation and cell proliferation assays (Supplementary Fig. S7E–S7G). This is consistent with the notion that BRD4 controls tumor growth through downstream targets other than Snail, including MYC (Fig. 2A).

Moreover, wild-type but not acetylation-deficient Snail mutants enhanced the migration and invasion of $BRD4^{+/+}$ cells (Supplementary Fig. S7H and S7I), which is likely due to stabilization of acetylated Snail by endogenous BRD4 in cells. Indeed, wild-type Snail and the acetylation-deficient mutants displayed no significant differences in migration and invasion capacities in $BRD4^{-/-}$ cells. These results suggest that BRD4 may preferentially recognize acetylated Snail and disrupt FBXL14- or β-Trcp1–mediated ubiquitination, thus stabilizing Snail to facilitate cancer invasion and metastasis.

The BRD4–Snail signaling axis regulates a subset of metastatic gene signature

We next assessed whether BRD4-mediated stabilization of Snail is pathophysiologically relevant to gastric tumorigenesis. IHC staining using gastric cancer tissues revealed a significant positive correlation of BRD4 and Snail expression, and an inverse correlation of Snail and β-Trcp1 or FBXL14 protein levels (Fig. 6C and D; and Supplementary Fig. S8A and S8B). Specifically, among the specimens with high levels of BRD4, more than 88% (75 of 85) showed high levels of Snail. However, in gastric cancer tissues with low levels of BRD4, only 38% (30 of 77) displayed high Snail expression ($R = 0.6353$). These results indicate that BRD4 may stabilize Snail in a subset of gastric cancers to promote tumor metastasis.

We analyzed transcriptome of $BRD4^{-/-}$ and $Snail^{-/-}$ cells to evaluate how the BRD4–Snail axis may impact on downstream signaling pathways. $BRD4^{-/-}$ cells upregulated 1,733 and downregulated 1,004 transcripts, whereas $Snail^{-/-}$ cells upregulated 407 and downregulated 112 transcripts (including mRNA and ncRNA, $P < 0.05$, fold change ≥ 1.5; Supplementary Fig. S9A and S9B). Deficiency of both BRD4 and Snail regulated several signaling pathways essential for tumorigenesis and metastasis (Supplementary Fig. S9C–S9F). Notably, 281 transcripts were regulated by both BRD4 and Snail as revealed by transcriptome analyses using $BRD4^{-/-}$ and $Snail^{-/-}$ cells (Fig. 6E), suggesting that BRD4 regulates more than half of Snail downstream targets. These overlapping downstream genes were enriched in pathways such as cytokine–cytokine receptor, Wnt signaling pathway, and Hippo signaling pathway (Fig. 6F). Quantitative PCR analyses confirmed that many overlapping metastasis-promoting genes were downregulated in the same trend in $BRD4^{-/-}$ and $Snail^{-/-}$ cells (Fig. 6G), as well as in cells treated with either Bromodomain inhibitors JQ1 or OTX015 (Supplementary Fig. S9G). These results collectively support the notion that elevated BRD4 expression in gastric cancer cells may contribute to Snail protein stabilization in a Snail acetylation–dependent manner by impeding FBXL14- or β-Trcp1 binding for Snail ubiquitination, thereby regulating Snail-associated proinvasive genes and cancer metastasis.

Discussion

Gastric cancer is the second leading cause of cancer-related deaths worldwide, and peritoneal and distant metastasis represents a major clinical challenge for curative surgery (25, 26). However, molecular targeted therapy is limited for gastric cancer patients with metastatic lesions, leading to overall survival of 3 to 6 months (27). Here, we identified the lysine acetylation reader

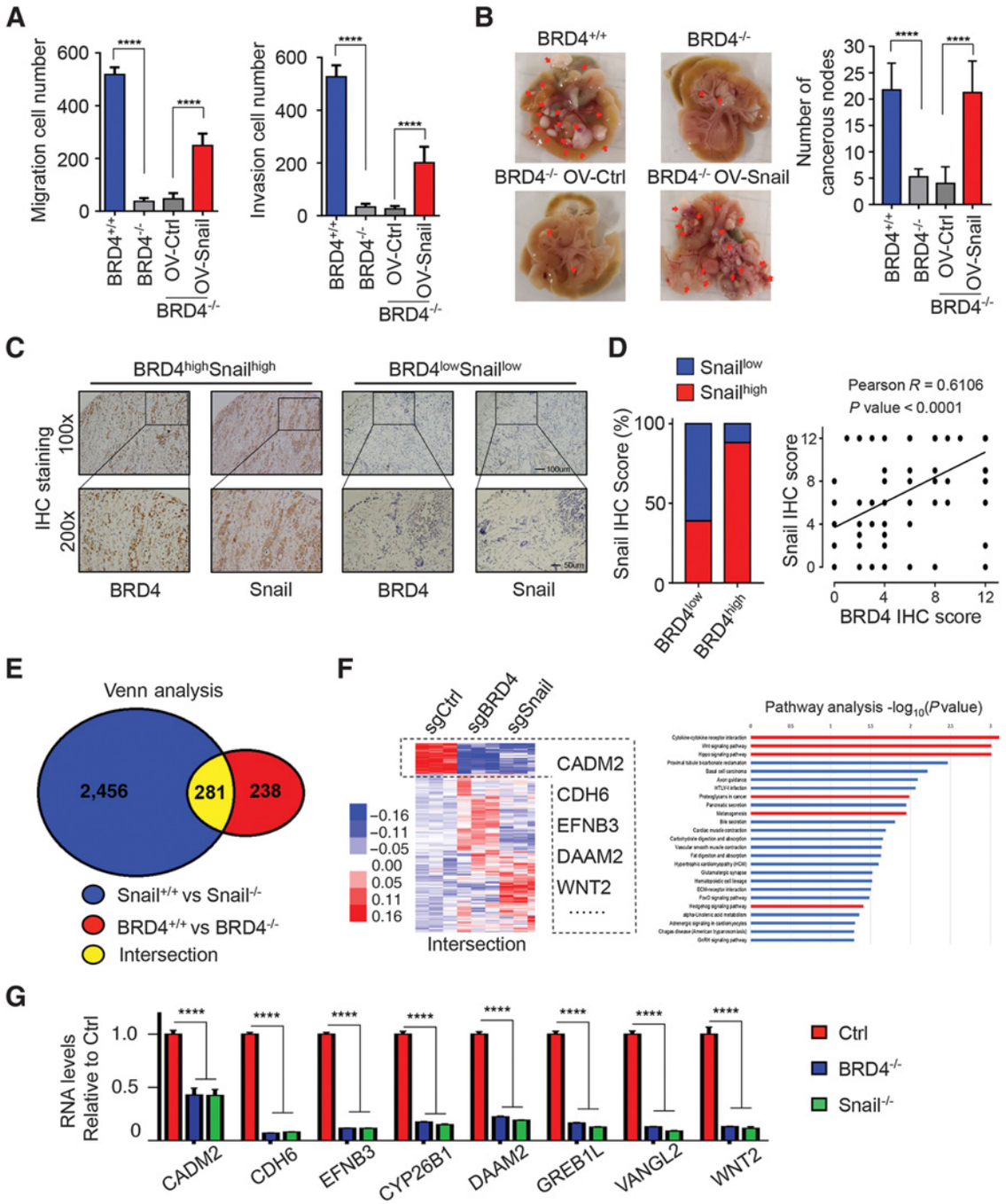

Figure 6.

BRD4-mediated stabilization of Snail contributes to cancer invasiveness and metastasis by regulating a partially shared metastatic gene signature. **A,** BRD4 promotes invasion of cancer cells through stabilizing Snail. Quantitative results of transwell migration and invasion assays using BRD4$^{+/+}$ and BRD4$^{-/-}$ HGC-27 cells, or BRD4$^{-/-}$ cells infected with control (OV-Ctrl) or Snail-expressing (OV-Snail) lentiviruses. Representative images are shown in Supplementary Fig. S7A. **B,** BRD4 enhances cancer metastasis through stabilizing Snail. Representative images of peritoneal metastatic nodules formed by BRD4$^{+/+}$ and BRD4$^{-/-}$ HGC-27 cells, or BRD4$^{-/-}$ cells infected with control or Snail-expressing lentiviruses. Hematoxylin and eosin–stained images of foci are shown in Supplementary Fig. S7B ($n = 5$ for each group). **C** and **D,** IHC images showing correlated expression pattern of BRD4 and Snail in gastric cancer tissues (**C**). The staining scores of BRD4 and Snail in 162 gastric cancer tissues were quantitatively analyzed in **D** ($P < 0.0001$). **E** and **F,** Venn diagrams illustrate the independent and overlapping transcriptome altered in BRD4$^{-/-}$ and Snail$^{-/-}$ HGC-27 cells (**E**). Heat maps and pathway analysis results of the transcripts in the overlapping part are shown in **F**, with cell metastasis pathways highlighted in red. **G,** BRD4 and Snail regulate a common subset of metastatic genes. Quantitative RT-PCR analysis of several metastasis-associated genes in BRD4$^{-/-}$ and Snail$^{-/-}$ HGC-27 cells. Representative images are presented (**B** and **C**). Quantitative results are presented as mean ± SEM (**A** and **B**) or mean ± SD (**G**). ****, $P < 0.0001$.

BRD4 as a promising therapeutic target for treating patients with metastatic gastric cancer. Specifically, we demonstrated that BRD4 is not only required for gastric cancer cell proliferation, but also essential for invasion and metastasis *in vitro* and *in vivo*. A role of BRD4 in cancer metastasis was recently implicated in the zinc finger MYND-type containing 8 (ZMYND8)-mediated control of HIF transcriptional activity (28) and Spermatogenic Zip 1 (SPZ1)–Twist1 complex-mediated cancer cell metastasis (29). BRD4 is a promising anticancer target as revealed by several loss-of-function genetic screens, and there are significant interests in development BET inhibitors for cancer therapy (30–35). Recent phase I clinical trials of BET inhibitors showed efficacy in a subset of patients with advanced hematologic malignancies or NUT carcinoma (31, 35). Although adverse effects of BET inhibitors have been observed, many of the side effects such as those of OTX015 are manageable and reversible with medical interventions (36). These results, together with our findings, suggest that BET inhibitors could be potentially applied to treat metastatic gastric cancer in clinical settings either alone or in combination with other drugs.

We found that BRD4 functions in a noncanonical posttranslational-dependent manner to regulate cancer biology. BRD4 was initially purified as a subunit of the Mediator complex that bridges transcriptional coactivators and RNA polymerase (Pol II; ref. 3). An N-terminal bromodomain of BRD4 recognizes acetylated histone tails, thereby coupling acetylation status of chromatin with gene transcriptional activity (3). Bromodomains also interact with other acetylated nuclear proteins (37). For example, bromodomain of BRD4 interacts with acetylated cyclin T1 (38), RelA (39), and TWIST (33) to modulate their transcriptional activity. However, whether and how BRD4 regulates its nonhistone binding protein stability remains unexamined. To this end, we identified acetylated Snail as a new binding partner of BRD4 and found that BRD4 binding stabilizes Snail by mitigating Snail ubiquitination through excluding its E3 ligases binding. This regulatory mechanism is essential for BRD4 to promote gastric cancer metastasis, as reintroducing Snail restored invasiveness and peritoneal dissemination of *BRD4*-depleted gastric cancer cells. Furthermore, transcriptome analysis demonstrated that BRD4 regulated more than half of the Snail-associated proinvasive gene signatures. Given that bromodomain exists in 46 proteins encoded by the human genome (37), further studies are warranted to investigate whether these bromodomain-containing proteins may also regulate stability of their interacting proteins to exert biological functions.

These findings represent an additional layer of regulation of Snail stability. As a short-lived protein, the stability of Snail is titrated by either K48-linked polyubiquitination (13–15) or monoubiquitination (40). Moreover, inflammatory cytokines such as TNFα also enhance CBP-mediated acetylation to stabilize Snail (18); however, the mechanism by which acetylation maintains the stability of Snail protein has remained unknown. We uncovered that acetylation of Snail enhanced its interaction with BRD4. BRD4 in turn competes with E3 ligases including FBXL14 and β-Trcp1 for Snail binding, resulting in impaired polyubiquitination and proteasomal degradation of Snail. Thus, the epigenetic reader BRD4 couples Snail acetylation to Snail stability, thereby promoting cancer invasiveness and metastasis.

In summary, the epigenetic reader BRD4 maintains the metastatic potential of gastric cancer through posttranslational stabilization of acetylated Snail. Given that overexpressions of both BRD4 and Snail are observed in multiple human cancers (5, 12), targeting the BRD4–Snail interaction by developed bromodomain inhibitors may be broadly applicable to prevent cancer metastasis in many types of cancers.

Disclosure of Potential Conflicts of Interest

No potential conflicts of interest were disclosed.

Authors' Contributions

Conception and design: Z.-y. Qin, Y.-l. Wei, D.-f. Chen, B. Wang
Development of methodology: T. Wang, P. Liu
Acquisition of data (provided animals, acquired and managed patients, provided facilities, etc.): Z.-y. Qin, T. Wang, S. Su, Q. Liu, L. Zhang, K.-w. Liu, X.-n. Zhang, L.-z. Wen, W.-j. Sun, Y. Guo, K.-j. Liu, L. Liu, X.-w. Wang, J. Wang, H.-l. Xiao, X.-w. Bian
Analysis and interpretation of data (e.g., statistical analysis, biostatistics, computational analysis): Z.-y. Qin, Y. Zhang, P. Liu, B. Wang
Writing, review, and/or revision of the manuscript: Z.-y. Qin, L.-t. Shen, G.-x. Zhu, B. Wang
Administrative, technical, or material support (i.e., reporting or organizing data, constructing databases): Y. Zhang, Z.-h. Zhou, Y.-l. Yao, H.-l. Xiao, X.-w. Bian, D.-f. Chen, B. Wang
Study supervision: D.-f. Chen, B. Wang

Acknowledgments

We thank Wei-guo Zhang (Department of Radiology, Daping Hospital, Army Medical University) for his kind support for animal MRI scanning. We thank Qiong Zhu (Department of Ultrasound, Xinqiao Hospital, Army Medical University, Chongqing, China) for her assistance in animal model. We also thank all the faculties in the Central Laboratory of Southwest Hospital (Army Medical University, Chongqing, China) for their kind support and administration.

This work was sponsored by the grants from the National Natural Science Foundation of China (NSFC Nos. 81822032 and 81872027 to B. Wang; 81672463 to D.-f. Chen), Natural Science Foundation of Chongqing, China (No. CSTC2016JCYJA0029 to X.-w. Wang), and Founding from the Army Medical University (2018XLC2023 to B. Wang and 2018XLC3059 to T. Wang).

The costs of publication of this article were defrayed in part by the payment of page charges. This article must therefore be hereby marked *advertisement* in accordance with 18 U.S.C. Section 1734 solely to indicate this fact.

Received February 4, 2019; revised June 6, 2019; accepted July 12, 2019; published first July 16, 2019.

References

1. Flavahan WA, Gaskell E, Bernstein BE. Epigenetic plasticity and the hallmarks of cancer. Science 2017;357.
2. Jones PA, Issa JP, Baylin S. Targeting the cancer epigenome for therapy. Nat Rev Genet 2016;17:630–41.
3. Fujisawa T, Filippakopoulos P. Functions of bromodomain-containing proteins and their roles in homeostasis and cancer. Nat Rev Mol Cell Biol 2017;18246–62.
4. Zuber J, Shi J, Wang E, Rappaport AR, Herrmann H, Sison EA, et al. RNAi screen identifies Brd4 as a therapeutic target in acute myeloid leukaemia. Nature 2011;478:524–8.
5. Delmore JE, Issa GC, Lemieux ME, Rahl PB, Shi J, Jacobs HM, et al. BET bromodomain inhibition as a therapeutic strategy to target c-Myc. Cell 2011;146:904–17.
6. Andrieu G, Belkina AC, Denis GV. Clinical trials for BET inhibitors run ahead of the science. Drug Discov Today Technol 2016;19:45–50.
7. Shang E, Wang X, Wen D, Greenberg DA, Wolgemuth DJ. Double bromodomain-containing gene Brd2 is essential for embryonic development in mouse. Dev Dyn 2009;238:908–17.
8. Houzelstein D, Bullock SL, Lynch DE, Grigorieva EF, Wilson VA, Beddington RS. Growth and early postimplantation defects in mice deficient for

the bromodomain-containing protein Brd4. Mol Cell Biol. 2002;22: 3794–802.
9. Muhar M, Ebert A, Neumann T, Umkehrer C, Jude J, Wieshofer C, et al. SLAM-seq defines direct gene-regulatory functions of the BRD4-MYC axis. Science 2018;360:800–5.
10. Lamouille S, Xu J, Derynck R. Molecular mechanisms of epithelial-mesenchymal transition. Nat Rev Mol Cell Biol 2014;15:178–96.
11. Moon H, Ju HL, Chung SI, Cho KJ, Eun JW, Nam SW, et al. Transforming growth factor-beta promotes liver tumorigenesis in mice via up-regulation of Snail. Gastroenterology 2017;153:1378–91.
12. Ni T, Li XY, Lu N, An T, Liu ZP, Fu R, et al. Snail1-dependent p53 repression regulates expansion and activity of tumour-initiating cells in breast cancer. Nat Cell Biol 2016;18:1221–32.
13. Zheng H, Shen M, Zha YL, Li W, Wei Y, Blanco MA, et al. PKD1 phosphorylation-dependent degradation of SNAIL by SCF-FBXO11 regulates epithelial-mesenchymal transition and metastasis. Cancer Cell 2014;26: 358–73.
14. Vinas-Castells R, Beltran M, Valls G, Gomez I, Garcia JM, Montserrat-Sentis B, et al. The hypoxia-controlled FBXL14 ubiquitin ligase targets SNAIL1 for proteasome degradation. J Biol Chem 2010;285:3794–805.
15. Zhou BP, Deng J, Xia W, Xu J, Li YM, Gunduz M, et al. Dual regulation of Snail by GSK-3beta-mediated phosphorylation in control of epithelial-mesenchymal transition. Nat Cell Biol 2004;6:931–40.
16. Wu Y, Wang Y, Lin Y, Liu Y, Wang Y, Jia J, et al. Dub3 inhibition suppresses breast cancer invasion and metastasis by promoting Snail1 degradation. Nat Commun 2017;8:14228.
17. Liu T, Yu J, Deng M, Yin Y, Zhang H, Luo K, et al. CDK4/6-dependent activation of DUB3 regulates cancer metastasis through SNAIL1. Nat Commun 2017;8:13923.
18. Hsu DS, Wang HJ, Tai SK, Chou CH, Hsieh CH, Chiu PH, et al. Acetylation of snail modulates the cytokinome of cancer cells to enhance the recruitment of macrophages. Cancer Cell 2014;26:534–48.
19. Wang T, Qin ZY, Wen LZ, Guo Y, Liu Q, Lei ZJ, et al. Epigenetic restriction of Hippo signaling by MORC2 underlies stemness of hepatocellular carcinoma cells. Cell Death Differ 2018;25:2086–100.
20. Wang T, Wu H, Liu S, Lei Z, Qin Z, Wen L, et al. SMYD3 controls a Wnt-responsive epigenetic switch for ASCL2 activation and cancer stem cell maintenance. Cancer Lett 2018;430:11–24.
21. Ran FA, Hsu PD, Wright J, Agarwala V, Scott DA, Zhang F. Genome engineering using the CRISPR-Cas9 system. Nat Protoc 2013;8:2281–308.
22. Wang B, Jie Z, Joo D, Ordureau A, Liu P, Gan W, et al. TRAF2 and OTUD7B govern a ubiquitin-dependent switch that regulates mTORC2 signalling. Nature 2017;545:365–9.
23. Kohnken R, Wen J, Mundy-Bosse B, McConnell K, Keiter A, Grinshpun L, et al. Diminished microRNA-29b level is associated with BRD4-mediated activation of oncogenes in cutaneous T-cell lymphoma. Blood 2018;131: 771–781.
24. Wang Z, Liu P, Inuzuka H, Wei W. Roles of F-box proteins in cancer. Nat Rev Cancer. 2014;14:233–47.
25. Bray F, Ferlay J, Soerjomataram I, Siegel RL, Torre LA, Jemal A. Global cancer statistics 2018: GLOBOCAN estimates of incidence and mortality worldwide for 36 cancers in 185 countries. CA Cancer J Clin 2018;68: 394–424.
26. Lordick F, Janjigian YY. Clinical impact of tumour biology in the management of gastroesophageal cancer. Nat Rev Clin Oncol 2016;13:348–60.
27. Van Cutsem E, Sagaert X, Topal B, Haustermans K, Prenen H. Gastric cancer. Lancet 2016;388:2654–64.
28. Chen Y, Zhang B, Bao L, Jin L, Yang M, Peng Y, et al. ZMYND8 acetylation mediates HIF-dependent breast cancer progression and metastasis. J Clin Invest 2018;128:1937–55.
29. Wang LT, Wang SN, Chiou SS, Liu KY, Chai CY, Chiang CM, et al. TIP60-dependent acetylation of the SPZ1-TWIST complex promotes epithelial-mesenchymal transition and metastasis in liver cancer. Oncogene 2019;38: 518–32.
30. Sun C, Yin J, Fang Y, Chen J, Jeong KJ, Chen X, et al. BRD4 inhibition is synthetic lethal with PARP inhibitors through the induction of homologous recombination deficiency. Cancer Cell 2018;33: 401–16.
31. Ozer HG, El-Gamal D, Powell B, Hing ZA, Blachly JS, Harrington B, et al. BRD4 profiling identifies critical chronic lymphocytic leukemia oncogenic circuits and reveals sensitivity to PLX51107, a novel structurally distinct BET inhibitor. Cancer Discov 2018;8:458–77.
32. Segatto M, Fittipaldi R, Pin F, Sartori R, Dae Ko K, Zare H, et al. Epigenetic targeting of bromodomain protein BRD4 counteracts cancer cachexia and prolongs survival. Nat Commun 2017;8:1707.
33. Shi J, Wang Y, Zeng L, Wu Y, Deng J, Zhang Q, et al. Disrupting the interaction of BRD4 with diacetylated Twist suppresses tumorigenesis in basal-like breast cancer. Cancer Cell 2014;25:210–25.
34. Asangani IA, Dommeti VL, Wang X, Malik R, Cieslik M, Yang R, et al. Therapeutic targeting of BET bromodomain proteins in castration-resistant prostate cancer. Nature 2014;510:278–82.
35. Dawson MA, Prinjha RK, Dittmann A, Giotopoulos G, Bantscheff M, Chan WI, et al. Inhibition of BET recruitment to chromatin as an effective treatment for MLL-fusion leukaemia. Nature 2011;478: 529–33.
36. Berthon C, Raffoux E, Thomas X, Vey N, Gomez-Roca C, Yee K, et al. Bromodomain inhibitor OTX015 in patients with acute leukaemia: a dose-escalation, phase 1 study. Lancet Haematol 2016;3: e186–95.
37. Filippakopoulos P, Picaud S, Mangos M, Keates T, Lambert JP, Barsyte-Lovejoy D, et al. Histone recognition and large-scale structural analysis of the human bromodomain family. Cell 2012;149:214–31.
38. Schroder S, Cho S, Zeng L, Zhang Q, Kaehlcke K, Mak L, et al. Two-pronged binding with bromodomain-containing protein 4 liberates positive transcription elongation factor b from inactive ribonucleoprotein complexes. J Biol Chem 2012;287:1090–9.
39. Huang B, Yang XD, Zhou MM, Ozato K, Chen LF. Brd4 coactivates transcriptional activation of NF-kappaB via specific binding to acetylated RelA. Mol Cell Biol 2009;29:1375–87.
40. Lee JH, Jung SM, Yang KM, Bae E, Ahn SG, Park JS, et al. A20 promotes metastasis of aggressive basal-like breast cancers through multi-monoubiquitylation of Snail1. Nat Cell Biol 2017;19:1260–73.